JOURNAL OF THERMOPHYSICS AND HEAT TRANSFER
Vol. 13, No. 1, January–March 1999

Startup Time Reduction in an Electrohydrodynamically Enhanced Capillary Pumped Loop

B. Mo,* M. M. Ohadi,† and S. V. Dessiatoun‡
University of Maryland, College Park, Maryland 20742
and
K. H. Cheung§
Naval Research Laboratory, Washington, D.C. 20375

The capillary pumped loop (CPL) is a state-of-the-art technique for cooling of spacecraft and telecommunication devices. It provides substantially higher cooling capacity than most heat pipes, more flexibility of installation, and much greater distance of heat transport because of the small diameter of wickless transport lines. Major disadvantages of the CPL are long and complicated startup procedures and the possibility of deprime at high heat input or load variation. The present work was an experimental study to characterize the start-up process for an electrohydrodynamically (EHD) assisted CPL system. Startup is achieved by establishing stable differential pressure and average temperature at the evaporator wall. When an electric field is applied to the evaporator wick, the liquid–vapor separation, the EHD pumping, and the instability-induced Maxwell stresses collectively contribute to reduce the startup time, as well as provide substantial improvement in CPL thermal performance. The experimental data in the present study show that at a power level of 10 W, the EHD can reduce the startup time by as much as 50% at an applied voltage of 10 kV. A similar trend is observed at power levels of 20 and 50 W.

Nomenclature

DP = differential pressure, kPa or psi
I = electric field current, A
i = heater's current, A
N = number of thermocouples
Q = power level, W
T = temperature, °C
V = heater's voltage, V
ϕ = electric field potential, kV

Subscripts
av = average
EHD = electric field
h = heater
total = total
w = evaporator wall

Introduction

THE capillary pumped loop (CPL), a wickless condenser heat pipe, is a passively pumped two-phase heat transport device that has demonstrated performance capabilities substantially greater than that of the conventional state-of-the-art heat pipes. For a CPL system, the most important design parameter, other than the steady-state maximum power capacity, is the transient startup process. Startup not only represents the highest stress on the evaporator wick, it also has a major impact on the design of the reservoir and its temperature controller, and on the overall effectiveness of the CPL to fulfill management of the thermal load. This paper investigates experimentally the reduction of CPL startup time with the assistance of the electrohydrodynamic (EHD) technique.

Received Nov. 21, 1997; revision received Sept. 3, 1998; accepted for publication Sept. 4, 1998.

*Research Assistant, Department of Mechanical Engineering.
†Professor, Department of Mechanical Engineering.
‡Associate Research Scientist, Department of Mechanical Engineering.
§Mechanical Engineer, Spacecraft Engineering Department.

The EHD is a new and promising technology that has demonstrated potential for significantly reducing the thermal system size/volume while providing on-line/on-demand control for the heat transfer surface. Its applicability for substantial heat transfer enhancement of industrially significant fluids such as refrigerants R-134a, R-123, PolyAlphaolefin, and certain aviation fuels has already been proven. Polarized EHD force (EHD pumping effect) also can assist or substitute capillary forces to collect, guide, and pump liquid condensate in regions of high electric field intensity, whereas the vapor component of the dielectric fluid is rejected to locations where the electric field is less intense. Because of the dominance of polarization EHD force over surface tension forces, the dielectrophoresis phenomenon may significantly improve the heat transfer capability of two-phase flow thermal devices, particularly for dielectric fluids with poor capillary forces. The EHD technique has high payoff potential and promising space and telecommunication applications, including its use in liquid-cooled thermal control systems and potential implementation in thermal management of almost all major subsystems. The terrestrial applications of the EHD technique are extensive and include commercial heat exchanger equipment for refrigeration and air conditioning, electronic cooling, cryogenic and process industry, and laser medical/industrial cooling applications.

Although high voltages may be required, because the magnitude of the electric current is very small (on the order of microampere in the present study), the EHD high-voltage power supply is small and introduces minimum additional cost to the system. Such power supplies are commonly used in household appliances such as color TVs and electrostatic air cleaners.

Because the magnitude of heat transfer enhancement in the EHD technique is directly proportional to the applied voltage, this provides an on-line/on-demand control feature to the heat transfer surface. This feature is particularly attractive for developing higher heat transfer capacity and vapor-tolerant CPL systems. EHD coupling will also enhance the CPL startup procedure and improve the heat transfer coefficient. All of these merits further promote readiness of CPL technology for space thermal control applications.

For a CPL system, the startup is identified by achievement of a steady temperature in the vapor line. Frozen startup refers to the heat input to the cold loop. The wick must be fully wetted, and the liquid zone in the evaporator should be cleared of bubbles before starting the CPL loop. This is usually accomplished by heating the reservoir and pressurizing the system to collapse all bubbles. Because the evaporator is the warmest part of the loop, collapsing the bubbles in that component requires filling the entire loop with liquid before allowing startup.

Previous published research work of relevance to the present study is very limited. Kiper et al.[1] and Cullimore[2,3] presented the startup transient analysis in a CPL system. Maidanik et al.[4] showed that the startup process could be characterized by three distinct periods. They also predicted the minimum heat capability for the reliable startup. Babin et al.[5] investigated an ion-drag pump-assisted capillary loop. Up to 100% improvement of the heat transport capacity and about 70 Pa of maximum EHD pressure head were reported. Bryan and Seyed-Yagoobi[6] studied the monogroove heat pipe with EHD pumping. A combination of the capillary and EHD forces yielded a 320-Pa pressure head at an applied potential of 20 kV. Ohadi et al.[7,8] investigated the feasibility of the EHD-assisted CPL system. Results of this experimental study identified the various characteristics of the startup process while reporting substantial improvement of the heat transfer coefficients in the evaporator wick of an EHD-assisted CPL system.

Experimental Apparatus

The schematic diagram of the EHD-assisted CPL setup used in the current experiments is shown in Fig. 1. The key component of the setup was the EHD-assisted evaporator. The maximum allowable heat transport capacity was designed for 1500 W. The working fluid was the environmentally accepted R-134a (HCHC134). Other major components included the cooling loop, the control (reservoir) loop, and the various auxiliary instrumentation for monitoring and control of the depriming conditions. A brief description of the main components of the experimental apparatus is given in the following text, with additional details available in Ohadi et al.[7,8]

EHD-Assisted Evaporator Test Section

An EHD-assisted evaporator was designed and fabricated to simulate conditions in a spacecraft CPL system. A 25.4-mm (1-in.) CPL pump (evaporator) was modified to realize the EHD-assisted test section. As shown in Fig. 2, a spring-type electrode was inserted into the liquid channel of the evaporator to implement EHD-assisted performance. The axial pitch of the spring electrode was about 1 mm. The o.d. of the spring was 8 mm, nearly the same as the i.d. of the wick structure. The grooved aluminum tubing served as the ground electrode, whose i.d. was 16 mm. A strip heater was placed at the surface of the evaporator to provide the required heating power. The outer surface area of the wick was 202 cm^2. A total of 14 thermocouples were mounted along the inside wall of the evaporator to measure the average wall temperature. Differential pressure measurement was used to evaluate the evaporator behavior in the loop. Seven additional thermocouples were probed in the loop to measure temperatures at various points in the loop, indicated by T in Fig. 1. The applied high-voltage electric field electrode was inserted in the liquid side of the wick. The voltage potential was applied via a laboratory-grade high-voltage power supply. The applied electric field promoted transfer of liquid across the wick to the evaporator surface.

Cooling (Condensing) Loop

The stability of the EHD-assisted CPL setup was maintained utilizing a cooling (condensing) loop. Cold water generated by a chiller (750 W capacity at $T = 5-10°C$) circulated in the condenser side and removed heat from the phase-change process in the evaporator. The amount of heat removal was controlled by adjusting circulating cooling water temperature. To achieve this, a temperature controller system was installed inside the chiller loop to maintain precise control of the chilled water temperature.

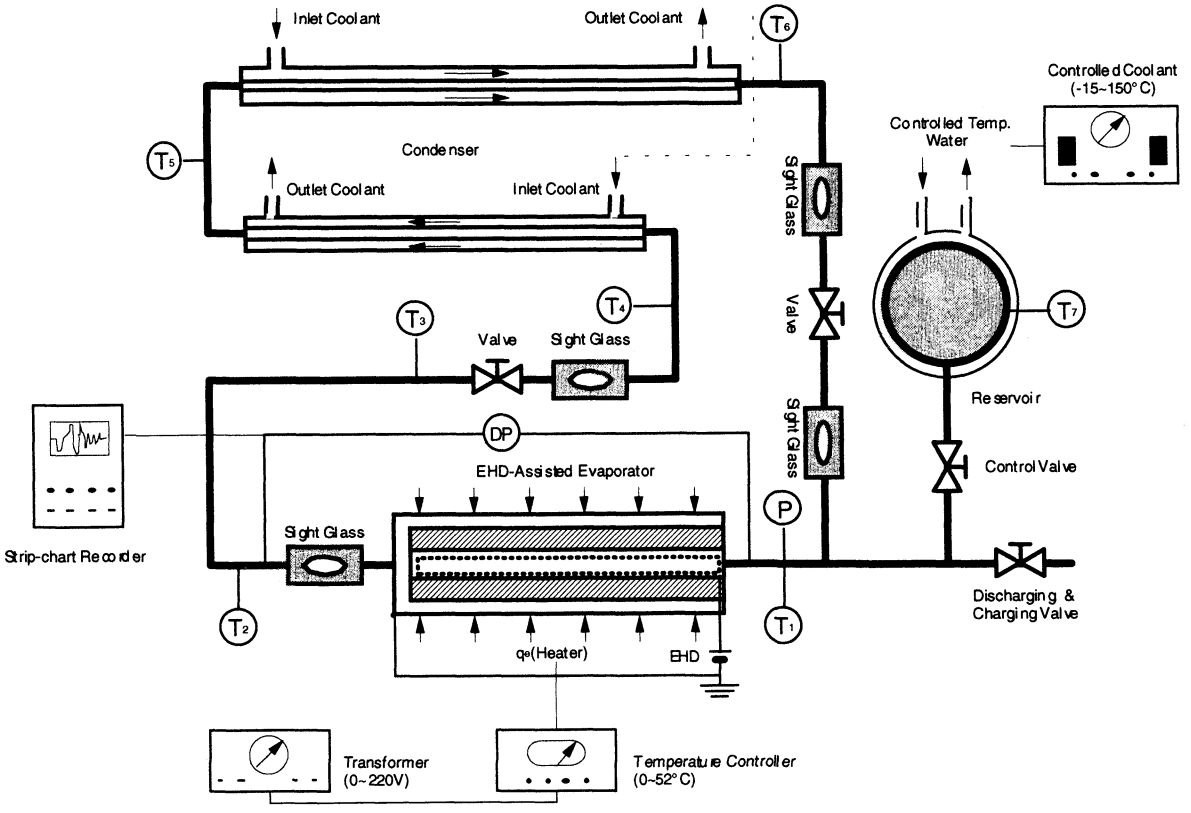

Fig. 1 Schematic of the EHD-assisted CPL.

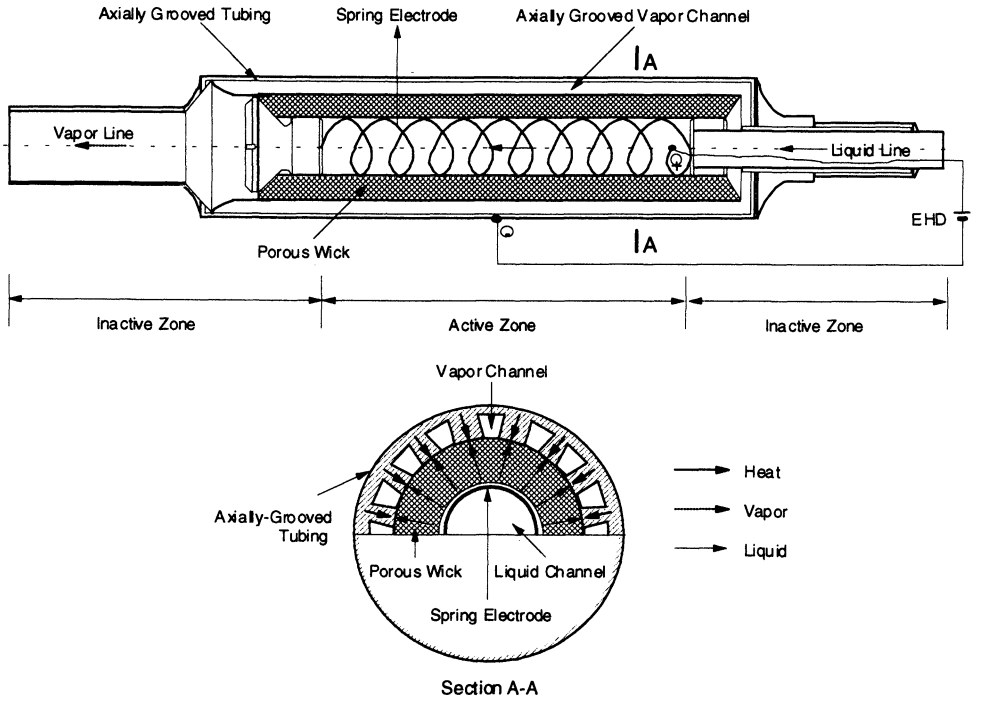

Fig. 2 Schematic of the EHD-assisted capillary evaporator.

Control (Reservoir) Loop

The function of the reservoir in the CPL system was to control the operating temperature and facilitate the startup procedure for the loop. Instead of an electric heater, a small chiller with temperature control was connected to the reservoir. The chiller was able to control the temperature in the range of −10 to 120°C. By setting the chiller temperature, a set reservoir temperature was maintained, thus fixing the operating temperature for the CPL system.

Depriming Condition Control

Two adjustable valves were installed on the liquid line and vapor line of the CPL loop, as shown in Fig. 1. At different power levels, by adjusting the opening of the two valves, the depriming conditions were triggered and the EHD-assisted control was realized. To better visualize the phenomenon, four custom-designed sight glasses were installed in the system to monitor the loop operation.

Experimental Procedure

A typical experimental procedure began by turning on the two-chiller systems. Chilled water circulated through the condenser for about a half-hour. At the same time, the controlled temperature of the reservoir was set at the operating temperature typically close to 25°C to push the liquid into the loop, and thus, wet the wick inside the evaporator. When the reservoir temperature reached the operating temperature, the heating power to the evaporator was applied to start up the CPL system. Then the various pressure transducer readings and temperatures at the evaporator wall and around the loop were monitored to ensure proper loop function. After the loop operation stabilized, the high-voltage electric field was applied to realize the EHD effect.

Next, the system was allowed to reach the steady-state conditions where fluctuations in wall temperatures, and the differential pressure (DP) average reading were less than 1%. After the steady-state condition was established, the local wall temperatures along the test section, the loop temperatures, and the high-voltage current were measured and recorded. Depending on the specific parametric study conducted, condition settings were changed accordingly to prepare for collecting the next data point. The procedure was repeated until completion of the experimental run.

Data Reduction

The average wall temperature of the evaporator was calculated using the following equation:

$$T_{\text{av}} = \sum_{i=1}^{N} T_{w,i}/N \tag{1}$$

where $T_{w,i}$ is the local wall temperature and N is the number of thermocouples (14) mounted on the evaporator wall.

The heat transfer rate of the test section (Q_h) was evaluated by

$$Q_h = V \times I \tag{2}$$

where V and I are the heater's applied voltage and current, respectively.

The ratio of EHD power consumption to the total heat transfer rate in the test section was calculated as

$$\frac{Q_{\text{EHD}}}{Q_{\text{Total}}} = \frac{Q_{\text{EHD}}}{Q_h + Q_{\text{EHD}}} \tag{3}$$

in which

$$Q_{\text{EHD}} = \phi \times i \tag{4}$$

where ϕ and i are electric field voltage potential and discharge current, respectively. The typical EHD power consumption (Q_{EHD}) for current experiments was on the order of 50 mW. When compared with the tested power input levels (Q_h, 10–50 W), the electrode power consumption was less than 0.5%, and thus, negligible.

The analysis of the system operational performance was achieved by collecting data at the DP, evaporator wall and loop temperatures, applied voltage and current, and other auxiliary measurements at various points in the loop.

The uncertainty calculations were based on the fact that a differential change of a function can be expressed in terms of the differential change of the dependent variables and the partial derivatives with respect to the corresponding dependent variables. Measurement errors for the current experiments were temperature ±0.20°C, differential pressure ±0.25% of the reading, heater voltage ±0.50% of the reading, heater current ±0.10% of the reading, applied EHD voltage ±0.10% of the reading, and applied EHD current ±0.10% of the reading. The calculated uncertainty in the average wall temperature was ±0.21°C. The calculations showed that uncertainty in the heat transfer rate (Q_h) was ±1.35 to ±4.25% and the uncertainty in power consumption (Q_{EHD}) was ±1.74 to ±5.16%, where the smaller uncertainty values were associated with the larger heat transfer rates.

Results

The average wall temperature and the differential pressure (difference between the outlet and inlet of the evaporator) for the base case (absence of an electric field) are shown in Fig. 3. As seen there, the startup process is classified to consist of three distinct regimes/zones.

Regime I

This regime takes place at the initial startup period and is characterized by a steady rise of temperature in the evaporator wall. At the beginning of this regime, the DP at the outlet and inlet of the evaporator is zero, or a very small amount, as a result of the absence of the vapor phase. After a certain amount of time has elapsed, the average temperature and DP increase to establish the incipient superheat for boiling, which is characterized by the sharp rise of DP before the process enters regime II.

Regime II

During this period, boiling of the working fluid in the evaporator takes place. Because of the vapor bubbles expansion and the heat removal associated with vaporization of the liquid inside the wick, this process is characterized by a quick drop of the differential pressure and average wall temperature.

Regime III

It is identified as the final stage of a successful startup process. During this period, the temperature of the evaporator wall and DP remain more or less constant. A gradual increase in vapor temperature at the outlet of the evaporator (vapor line) and a decrease in liquid temperature at the inlet of the evaporator (liquid line) takes place as a result of the fluid circulation in the loop. Finally, the loop reaches its stable operational state.

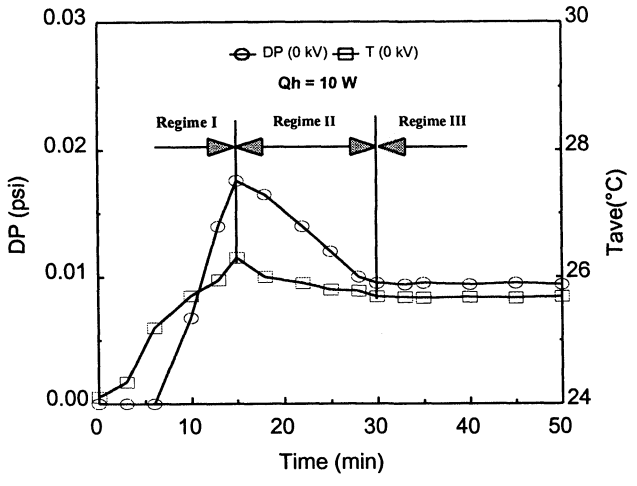

Fig. 3 Distinct regimes during the startup process.

To address the transient nature of the process, the DP data were recorded continuously with a strip-chart recorder and the 14 wall temperatures were collected and recorded approximately every 3 min. We repeated the experiments at least twice to verify repeatability of the experimental data.

Figure 4 provides a comparison of the data for the base case (0-kV applied voltage) and in the presence of the EHD effect (10-kV applied voltage). From the data in Fig. 4, it is clear that, as a result of the electric field effect, the startup time is considerably reduced. Moreover, as seen in the figure, the data indicate that the DP and temperature curves exhibit a similar trend with time variation. At a power (heat load) level of 10 W, the startup time is reduced from 30 min to 15 min at an

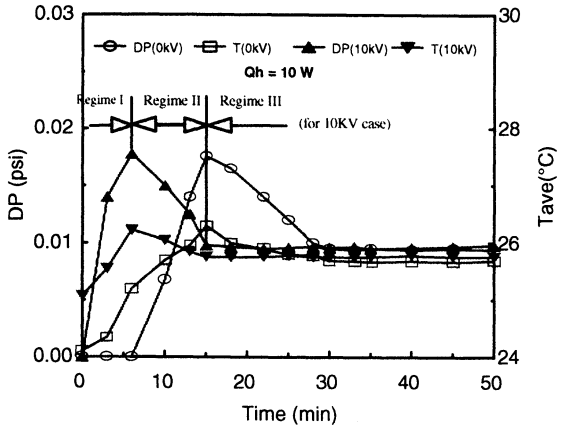

Fig. 4 Reducing startup time with EHD at 10 W.

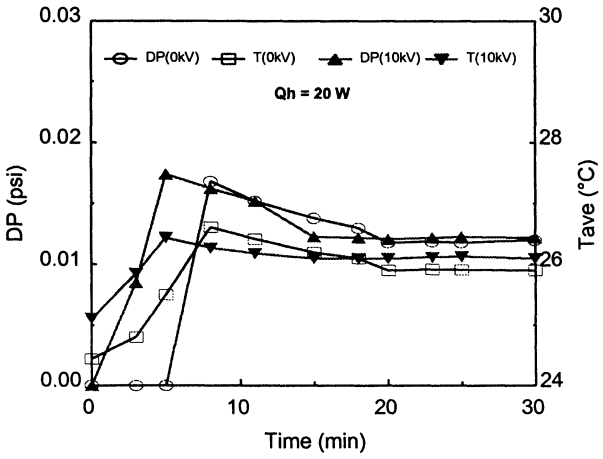

Fig. 5 Reducing startup time with EHD at 20 W.

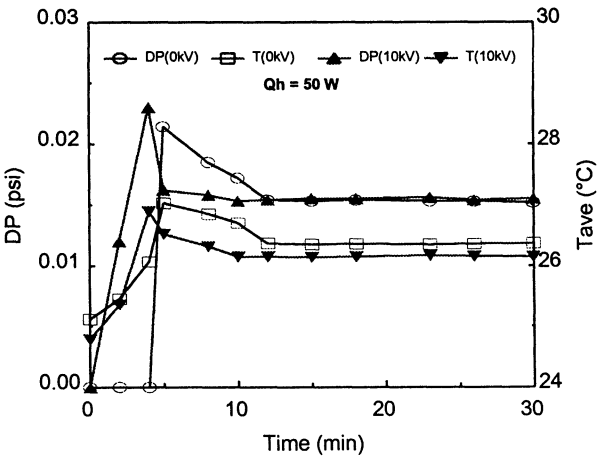

Fig. 6 Reducing startup time with EHD at 50 W.

applied voltage of 10 kV. The incipient superheat for boiling is the key parameter for the startup process. During the base case, the required incipient superheat for boiling occurs after 15 min. However, the EHD effects speed up the occurrence of the incipient superheat to about 6 min at the 10-kV applied voltage.

Performance improvements similar to that of the 10-W power level were achieved at power levels of 20 and 50 W, illustrated in Figs. 5 and 6, respectively. At an applied voltage of 10 kV, the startup time was reduced by about 30% for the 20-W and 20% for the 50-W power level. The results indicate that the EHD-assisted startup time reduction is less significant at higher power levels. This is because the menisci form more easily at high heat load levels and produce a higher capillary force. Therefore, the relative effectiveness of EHD force for the startup time reduction becomes less pronounced.

Attention is next brought to Fig. 7, where the typical electrode power consumption is depicted. An overview of the results in Fig. 7 suggests that in a worst-case scenario, the power consumptions are less than 30 mW. When compared with the wick heat transfer rate (10 W), the EHD power consumption is less than 0.3%, thus being negligible. Though not shown here, similar trends were observed for the power levels of 20 and 50 W.

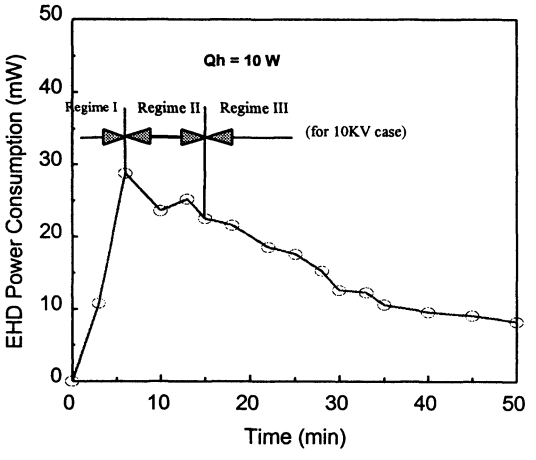

Fig. 7 EHD power consumption (Q_{EHD}) at 10 W.

Discussion

Under the base case (0-kV applied voltage, Fig. 3), the evaporator wick needs the initial time period to develop the menisci to produce the capillary force. The first period (regime I) is therefore characterized by the gradual temperature rise at the evaporator wall and a nearly zero DP at the beginning, for example, the first 7 min in Fig. 3. The next period (regime II) is followed by generating vapor bubbles first at the inner surface of the wick (see Fig. 8a). Regime II is characterized by the peak wall temperature and differential pressure at the beginning, followed by a sharp drop. As a result of the evaporation process, the latent heat of vaporization causes rapid heat removal from the wick, leading to a sharp drop of the DP and wall temperature. Finally in regime III, the temperature and differential pressure reach a nearly stable condition and serve to establish the successful startup process.

When an electric field is applied to the CPL system (Figs. 4–6), three factors contribute to the EHD-enhanced mechanism of reducing the startup time: EHD-influenced modified bubble formation, EHD pumping effect, and EHD-induced instability phenomenon. These contributing effects are briefly discussed in the following text.

It is well established that the fluid with a higher dielectric constant will always move toward the stronger electric field strength zones and vice versa.[9] This serves to accelerate bubble formation in the wick vapor channel away from the electrode. With regard to the pumping effect, when applying high voltage in the liquid phase, the electric field will generate an electric force density that leads to pumping of the liquid. Melcher[10] gives the expression for such pumping phenomenon. The third major EHD contribution effect, particularly for phase-change processes, is caused by the liquid–vapor interface instability. The interfacial electric stress either pulls or pushes the interface, depending on the gradient and direction of the applied electric field strength. For two-phase flow processes, the EHD forces are much stronger because of the difference in dielectric

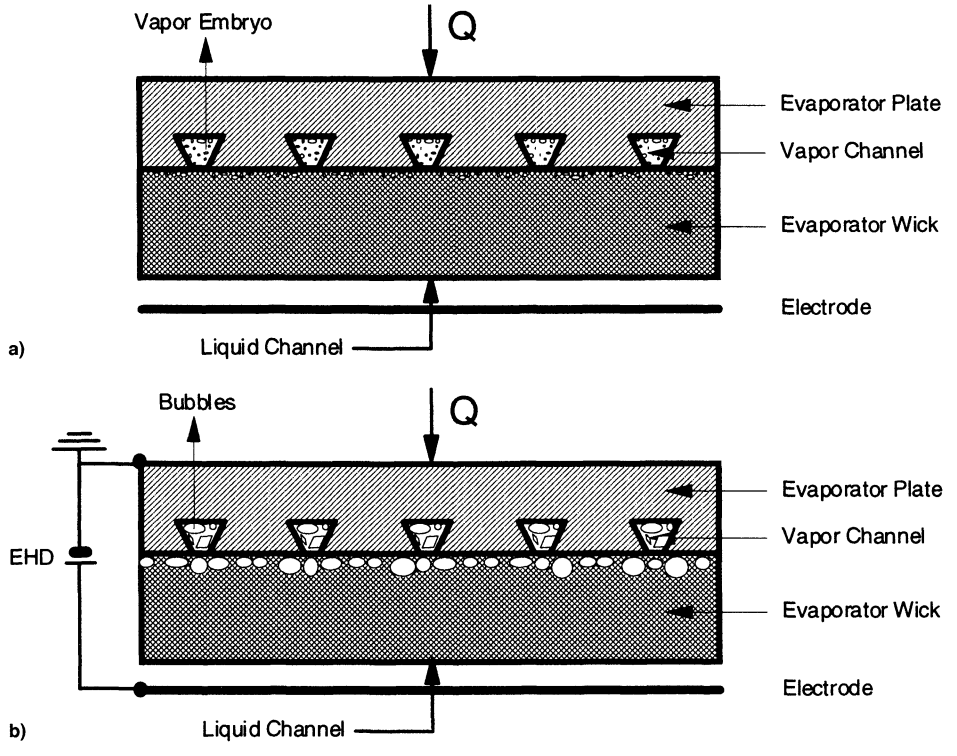

Fig. 8 EHD-reducing startup time for a CPL system. In the a) absence and b) presence of EHD.

constants of liquid and vapor phases. At the liquid–vapor interface, the dielectric constant takes a singularity, thus causing a favorable interfacial instability that generates Maxwell stresses. These stresses in turn cause the interface to move in the direction of reduced electric field intensity (vapor zone) caused by induced electric pressures.

Figure 8 schematically depicts the wick behavior for the base case and in the presence of the applied voltage. It illustrates the EHD effects on vapor embryos and bubbles. Observations suggest that EHD effects accelerate the process from vapor embryos to bubbles, thus reducing the required time for occurrence of the incipient superheat. The EHD force acts in the same direction as the capillary force to augment the pumping effect. This has been verified in an earlier feasibility study,[7] which reported EHD augmentation of liquid pumping through the wick structure. However, the study could not quantify the relative contribution of EHD vs capillary forces. In a separate study, Ohadi et al.[8] showed that the capillary force was a major driving force for the EHD-assisted CPL. The EHD effects helped the capillary force and enhanced the heat transfer coefficient by nearly three times.

Conclusions

The present work was an experimental study to characterize the startup process for a CPL system. The startup process was identified by establishing an almost stable differential pressure and average wall temperature in the evaporator. When an electric field is applied, EHD-induced modified bubble formation effect and the EHD pumping phenomenon influence the process by speeding up attainment of the incipient superheat required for the onset of evaporation. Thus, less time is needed to develop the menisci in regime I. After regime I, the instability-induced EHD pumping at the liquid–vapor interface pushes the liquid–vapor interface up to near the evaporator wall, leading to enhanced phase-change heat transfer. These EHD-enhanced mechanisms collaborate to reduce the required durations of the three different regimes involved. Experimental data showed that a nearly 50% startup time reduction was achieved at a low power level of 10 W at an applied voltage of 10 kV. The startup time reduction for the 20- and 50-W power levels were 30 and 20%, respectively.

Acknowledgments

Financial support of this work by a consortium of sponsoring members is gratefully acknowledged. Technical assistance and laboratory support by the Swales Aerospace Inc., Beltsville, Maryland, and the efforts of Eric Haught and Marc Kaylor in this regard, were particularly essential to successful completion of this work.

References

[1]Kiper, A., Feric, G., Anjum, M., and Swanson, T.D., "Transient Analysis of a CPL Heat Pipe," AIAA Paper 90-1658, June 1990.

[2]Cullimore, B. A., "Start Up Transients in CPLs," AIAA Paper 91-1374, June 1991.

[3]Cullimore, B. A., "Capillary Pumped Loop Application Guide," Society of Automotive Engineers, Paper 932156, July 1993.

[4]Maidanik, Y., Solodovnik, N., and Fershtater, Y., "Experimental and Theoretical Investigation of Startup Regimes of Two-Phase Capillary Pumped Loops," Society of Automotive Engineers, Paper 932305, July 1993.

[5]Babin, B. R., Peterson, G. P., and Seyed-Yagoobi, J., "Experimental Investigation of an Ion-Drag Pump-Assisted Capillary Loop," *Journal of Thermophysics and Heat Transfer*, Vol. 7, No. 2, 1993, pp. 340–345.

[6]Bryan, J. E., and Seyed-Yagoobi, J., "Heat Transport Enhancement of Monogroove Heat Pipe with Electrohydrodynamic Pumping," *Journal of Thermophysics and Heat Transfer*, Vol. 11, No. 3, 1997, pp. 454–460.

[7]Ohadi, M., Dessiatoun, S., Mo, B., Kim, J., Cheung, K., and Didion, J., "An Experimental Feasibility Study on EHD-Assisted Capillary Pumped Loop," *Space Technology and Applications International Forum, American Institute of Physics Conference Proceedings 387*, AIP Press, Woodbury, NY, 1997, pp. 567–572.

[8]Ohadi, M., Dessiatoun, S., and Mo, B., "An EHD-Assisted Capillary Pumped Loop," Progress Rept. 6, EHD Aerospace Consortium, Enhanced Heat Transfer Lab., Univ. of Maryland, College Park, MD, Feb. 1997.

[9]Pohl, H. A., *Dielectrophoresis—The Behavior of Neutral Matter in Non-Uniform Electric Fields*, Cambridge Univ. Press, New York, 1965.

[10]Melcher, J. R., *Continuum Electromechanics*, MIT Press, Cambridge, MA, 1981.